

Combining pulse compression and adaptive drive signal design to inverse filter the transducer system response and improve resolution in medical ultrasound

S. Venkatraman N. A. H. K. Rao

Centre for Imaging Science, Rochester Institute of Technology 54 Lomb Memorial Drive, Rochester, NY 14623-5604, USA

Abstract—An adaptive inverse filtering technique has been incorporated into a medical ultrasound B-scan scheme that used a linear frequency modulated pulse for imaging. Resolution improvement is demonstrated with imaging experiments on wire targets and tissue-mimicking phantoms.

Keywords—Frequency modulation, Inverse filtering, Pulse compression, Speckle, Ultrasonic imaging

Med. & Biol. Eng. & Comput., 1996, 34, 318–320

1 Introduction

WE HAVE examined theoretically and demonstrated experimentally how linear frequency modulation (FM) and pulse compression can be incorporated into a prototype medical ultrasound imaging system (RAO, 1994; RAO *et al.*, 1995). Instead of a short impulse excitation, a longer duration (20 μ s) uniform amplitude linear frequency modulated drive signal is used as input to the transducer. The frequency is swept beyond the 20 dB bandwidth of the transducer and is centred on its resonant frequency f_0 (POLLAKOWSKI and ERMERT, 1994). The transducer imposes its own amplitude modulation on the

reflected FM signal. The crosscorrelation (matched filtering) processing of the reflected FM signal with the reference FM signal results in a compressed pulse.

The 6 dB pulse width, computed on the envelope of the compressed pulse, defines the axial resolution. This axial resolution depends inversely on the 6 dB bandwidth Δf of the transducer, which is generally about 50% of its operating centre frequency f_0 . Thus to improve resolution, we have to work with a higher f_0 transducer, consequently decreasing the penetration depth because attenuation in soft tissue increases with frequency (RAO, 1994). Increasing the effective Δf of a low f_0 transducer, by amplitude pre-enhancement of the FM drive signal is useful in improving resolution and the time-bandwidth product of the matched filter.

An adaptive technique that derives the pre-enhancement signal in a feedback loop has been developed and is described in this paper. It has been incorporated into a prototype digital B-scan imaging system, and the resolution improvement is demonstrated with experiments on clinically relevant phantoms. Although the technique performs inverse filtering, it is operationally different from deconvolution or Wiener optimal inverse filtering, which is normally applied as a post-processing step on the reflected signal. The performance of the latter is generally limited by noise.

2 Method

A block diagram of the integrated imaging system is shown in Fig. 1, with the PC as the controller. Experiments were performed using a focused transducer (focal length 5 cm) with a centre frequency of 2.25 MHz and a 6 dB bandwidth of 1.2 MHz. Water-filled and tissue-mimicking phantoms are scanned with a wire target at 5 cm. The input to the transducer

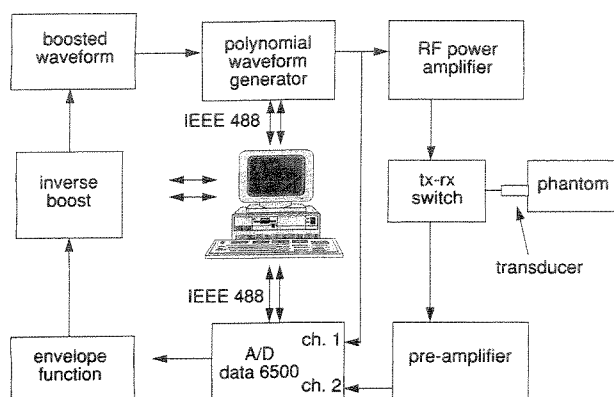


Fig. 1 Experimental set-up

First received 30 November 1995

© IFMBE: 1996

is from an arbitrary waveform generator that calculates the waveform specified by eqn. 1 at time intervals of 10 ns, and outputs it to the power amplifier that drives the transducer.

$$P(t) = \sin \left[2\pi \left\{ \left(f_0 - \frac{B}{2} \right) t + \left(\frac{B}{2T_0} \right) t^2 \right\} \right]; 0 \leq t \leq T_0 \quad (1)$$

The instantaneous frequency of the uniform amplitude FM signal is swept linearly with time, from $(f_0 - B/2)$ to $(f_0 + B/2)$ over a time period $T_0 = 20 \mu\text{s}$. f_0 is set at 2.4 MHz and B at 1.8 MHz in order to drive the transducer beyond its 20 dB bandwidth. Note that the amplitude (envelope) of $P(t)$ is uniform over the time interval T_0 , although the beginning and end portions of the pulse are smoothly decreased to zero with a 10th-order Butterworth weighting function to minimise the transient response.

The transducer is moved with a stepper motor at 0.15 mm intervals to 100 different lateral positions, and the reflected 1-D FM signal at each location is digitised* at 50 MHz with 8 bit resolution. Fig. 2a is the reflected FM signal for all lateral positions shown as a 2-D grey-scale image. The amplitude reduction at low and high frequencies due to the finite bandwidth of the transducer is visible. The horizontal cut through the centre of Fig. 2a represents the reflected FM signal $r(t)$ when the transducer is right on top of the wire target. This 1-D signal $r(t)$ carries information about the frequency response of the transducer and is used adaptively to derive an inverse boost function for the second pass. The $r(t)$ signal is first crosscorrelated with $P(t)$, the constant amplitude FM drive signal, to estimate any residual time shift needed to align it. The envelope detected signal $A(t)$ is obtained from $r(t)$ using the Hilbert transform.

The data are downloaded from the digitiser to the PC via the IEEE 488 interface. The inverse boost envelope function $A^{-1}(t)$ is calculated using the software and multiplied with the constant amplitude FM signal $P(t)$ to produce the new drive signal (inverse amplitude boosted pulse) for the second pass. This function is then uploaded into the waveform generator via the IEEE 488 interface.

* Analogic Corporation DATA 6500

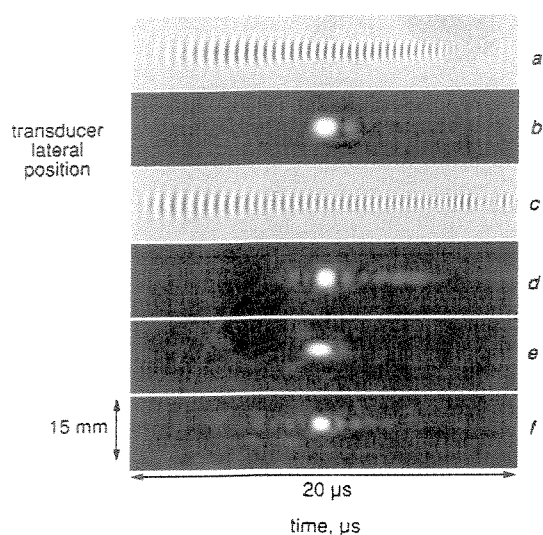


Fig. 2 Results on wire targets: (a) reflected FM from first pass in water; (b) PSF after pulse compression from first pass in water; (c) reflected FM from second pass in water; (d) PSF after pulse compression from second pass in water; (e) PSF after first pass in attenuating phantom; (f) PSF after second pass in attenuating phantom

The reflected signal from the second pass is shown in Fig. 2c. The amplitude boost at the low and high frequencies and amplitude equalisation are visible in the 2-D image. The pulse compression step is accomplished by crosscorrelating every horizontal line of the reflected signal with $P(t)$ as the reference signal. Finally, envelope detection is performed using the Hilbert transform on each line.

The final 2-D PSF (point spread function) is shown in Fig. 2b, for the first pass (without inverse filtering) and in Fig. 2d after the second pass (with inverse filtering). Similar experiments are performed on wire targets embedded in a tissue-mimicking phantom† with attenuation coefficient $\alpha_0 = 0.5 \text{ dB} (\text{cm MHz}^{-1})$. The final PSF is shown in Figs. 2e and f for the first and second passes, respectively, for the attenuating case. The same phantom also contains 1.5 cm diameter speckle contrast disks embedded in a speckle generating background. The disk centres are located 5 cm from the transducer. Only the disks with a speckle contrast of -15 dB and -6 dB relative to the background are scanned, and images are acquired with conventional short pulse, FM pulse without inverse filtering and FM pulse with inverse filtering. In all experiments performed on the tissue-mimicking phantom, the inverse boost function is identical to that adaptively derived for the water phantom.

3 Results

In Fig. 2 the 6 dB width of the 2-D PSF is measured in the axial (horizontal) and lateral (vertical) directions defining the axial and lateral resolutions for all four cases. The axial resolution improves from $1.06 \mu\text{s}$ to $0.82 \mu\text{s}$ in the non-attenuating case (compare Fig. 2b and 2d) and from $1.016 \mu\text{s}$ to $0.801 \mu\text{s}$ in the attenuating case. This is a direct consequence of increasing the bandwidth beyond the 6 dB bandwidth of the transducer by the inverse boost step. It is important to note that the conventional impulse excitation of the transducer will only produce resolution similar to the first pass results. There is a small trade-off in terms of increased sidelobe levels along the axial direction, as seen in Fig. 2d.

The lateral resolution, not affected by this process, is 3.3 mm for the first and second passes in the non-attenuating medium and 2.25 mm in the attenuating medium. Improvement in lateral resolution here is encouraging, but the reason is not obvious. Note that as the inverse boost function is the same as that derived for the water phantom, we have inverse filtered only the transducer's frequency response, and not that of the attenuating medium.

Fig. 3 shows three final images from experiments performed on the speckle contrast disks. Fig. 3a is from a conventional

† Model 539, ATS Laboratory Inc.

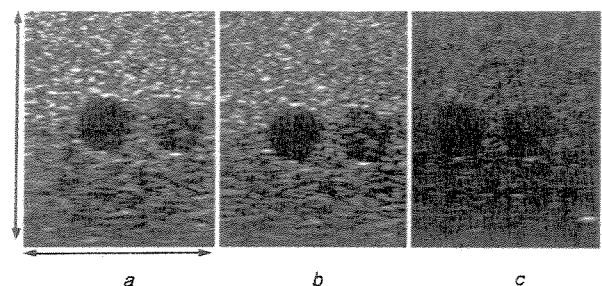


Fig. 3 Imaging results on speckle contrast phantom: (a) short pulse, (b) FM pulse without inverse filtering, (c) FM pulse with inverse filtering

short pulse, Fig. 3*b* is from an FM pulse (first pass, without inverse filtering) and Fig. 3*c* is from an FM pulse (second pass, with inverse filtering). The image size of each panel is 6 cm × 4.5 cm. The speckle texture in Figs. 3*a* and *b* is very similar, determined mainly by the transducer response. Fig. 3*c* and has a much finer texture with an average speckle spot size much smaller than in Figs. 3*a* and *b*. This is mainly due to the improvement in the axial resolution resulting from our inverse filtering step.

4 Conclusions

In summary, we have presented a prototype experimental ultrasonic imaging system with FM pulse excitation and a feedback loop to perform adaptive inverse filtering. The outcome is an improvement in the effective bandwidth and hence the resolution that is otherwise not possible with a conventional impulse-driven system. We have also demonstrated an improvement in the speckle texture pattern. Smaller speckle spot size will help improve the low contrast lesion detectability. The technique could be used to inverse filter the frequency-depen-

dent attenuation of soft tissue also in addition to the transducer response.

Acknowledgments—This work was supported in part by a grant from the Whitaker Foundation.

References

- RAO, N., MEHRA, S., BRIDGES, J. and VENKATARAMAN, S. (1995): 'Experimental point spread function of FM pulse imaging scheme,' *Ultrasonic Imaging*, **17**, pp. 114-141
- RAO, N. (1994): 'Investigation of a pulse compression technique for medical ultrasound: a simulation study,' *Med. Biol. Eng. & Comput.*, **32**, (2), pp. 181-188
- POLLAKOWSKI, M. and ERMET, H., (1994): 'Chirp signal matching and signal power optimization in pulse-echo mode ultrasonic nondestructive testing,' *IEEE Trans.*, **UFFC-41**, pp. 655-659
- RAMAN, R., and RAO, N. (1994): 'Pre-enhancement of chirp signal for inverse filtering in medical ultrasound.' Proc. 16th Int. Conf. of IEEE Engineering in Medicine and Biology Society, Baltimore, Maryland, Vol. 1, pp. 676-677